Theoretical and Applied Climatology (2021) 144:25–37
https://doi.org/10.1007/s00704-020-03512-w

ORIGINAL PAPER

Seasonal trend analysis of minimum air temperature in La Plata river basin

Marisa G. Cogliati[1] · Gabriela V. Müller[2] · Miguel A. Lovino[2]

Received: 25 February 2020 / Accepted: 28 December 2020 / Published online: 9 January 2021

Abstract

Regional economies that depend predominantly on agriculture and livestock are heavily affected by changes in air temperature, one such case are the activities in La Plata river basin (LPB). Some studies suggest that variations in the seasonal cycle and season onset would affect efficiency in the use of radiation by vegetation. This paper evaluates the distribution of minimum temperature seasonality trends over LPB, describes the trends in the seasonal cycle, and detects changes of minimum temperature extremes characterized by the number of frost days and the frequency of warm and cold nights. The analysis includes absolute minimum temperature 0(TnMin) and minimum average temperature (TnMean) from ERA5 reanalysis for the 1980–2015 period. Significant positive trends in the amplitude of annual average TnMin and TnMean are observed over more than half the area (53.5% and 69.9% of the basin, respectively). Amplitude and phase parameters suggest that average minimum temperature underwent greater variation than absolute minimum temperature over LPB. The shifts in phase indicate that minimum temperatures occurred earlier than usual in the year considering the 35-year series. In general terms, there is a shift toward warmer conditions. This warming is evident in seasonal trends of minimum temperature as well as in the significant increase in the number of warm nights, a significant decrease of cold days and a significant decrease in the number of frost days in the highest Andes mountains in the west of the LPB.

Keywords Seasonal temperature trends · Warm nights · Cold nights · Frost days · ERA5 · South America

1 Introduction

La Plata river basin (LPB) is home to abundant high-quality natural resources and high productivity. LPB includes the cereal production areas of Argentina, Brazil, Uruguay, Paraguay, and Bolivia. It produces 90% of Argentina's cereal and oil crops; 30% of Brazil's rice, soybeans, wheat, and maize; almost the entire cereal and oil crop production of Uruguay and Paraguay; and the main crops of Bolivia (Barros et al. 2006; CIC 2017). This turns the LPB into one of the most important regions in South America, from both the environmental and the economical perspectives. Regional economies that depend so heavily on natural resources and ecosystem services are subject to weather and climate variability.

In terms of climate variability, the main variables that affect crops are temperature (Sadras and Monzón 2006; García et al. 2016; among others) and precipitation (Penalba et al. 2007; Müller et al. 2011, among others). Precipitation variability can affect soybean and corn crops, which are widespread in LPB (Lee and Berbery 2012). For instance, precipitation has a strong correlation with the yields of soybean and corn in the south of Brazil (Berlato et al. 2005) and in Paraguay (Mayeregger et al. 2015). Extreme rains strongly influence the variability in soybean yields in central-eastern Argentina, a region known as the Humid Pampa (Penalba et al. 2007). Increased precipitation during spring, mainly associated with El Niño (Berri and Bertossa 2004), increases soybean and

✉ Marisa G. Cogliati
marisa.cogliati@fahu.uncoma.edu.ar

Gabriela V. Müller
gvmuller@fich.unl.edu.ar

Miguel A. Lovino
mlovino@unl.edu.ar

[1] Departamento de Geografía. Facultad de Humanidades, Universidad Nacional del Comahue, Av. Argentina, 1400 Neuquén, Argentina

[2] Consejo Nacional de Investigaciones Científicas y Técnicas (CONICET), CEVARCAM, Facultad de Ingeniería y Ciencias Hídricas, Universidad Nacional del Litoral, Santa Fe, Argentina

corn yields. Droughts, that may be associated with La Niña events, reduce crop yields in the Humid Pampa, southern Brazil (Arsego et al. 2018), and Paraguay (Mayeregger et al. 2015). Temperature also plays an important role in crop development; for example, it may shorten crop cycles, such as wheat (Sadras and Monzón 2006). Both precipitation and temperature control the efficiency with which vegetation makes use of solar radiation, and, therefore, they control net primary productivity as well (Piñeiro et al. 2006).

In the last decades, the mean and extreme values of precipitation and temperature have changed. Temperature extremes are shifting toward warmer conditions in southeastern South America (Alexander et al. 2006; Carril et al. 2016), and in particular, minimum temperature has been increasing since 1960 (Magrin et al. 2014; Lovino et al. 2018a). Warmer minimum temperatures have larger impacts on grain yields than on vegetative growth, because they lead to an increase in the senescence rate and a consequent drop in the ability of crops to fill their grains and fruits (Hatfield and Prueger 2011).

Increased minimum temperature and water availability, along with technological improvements, explain the higher yields of cereals and oilseeds in the most productive regions, such as the Humid Pampa (Magrin et al. 2014; Müller et al. 2011; Fernández Long et al. 2013). In this region, rising minimum temperature has caused the number of warm days and nights to increase; in addition, a decrease was observed in the number of cold days and nights (Skansi et al. 2013; Magrin et al. 2014; Lovino et al. 2018b). The rise in night temperature leads to a shortening of growth phases such as the filling of wheat grains. As a consequence, production loss is about 3% per degree of average temperature rise in the Humid Pampa (García et al. 2015, 2016). Warmer minimum night temperatures affect the pollination period of wheat and barley. In particular, during the critical period for wheat (approximately between 20 days before and 10 days after flowering), production losses are approximately 7% per degree above mean minimum temperature (Magrin et al. 2014; García et al. 2015). Nocturnal warming during the post-anthesis period (when plants bloom and become fertilized allowing seed production) has direct effect on wheat grain weight (García et al. 2016). A noticeable increase in minimum temperature during the wheat growing cycle (July to December), mainly in October and November, caused drops in average production of 28.3 kg/ha/year during the 1930–2000 period and 52.7 kg/ha/year during the 1970–2000 period in the Humid Pampa region (Magrin et al. 2014). Thus, rising minimum temperatures and warmer nights disrupt the critical periods for wheat and barley crops, entailing significant potential yield losses mainly due to less accumulated radiation as a consequence of shorter critical periods (Verón et al. 2015).

Understanding the variability, extremes, and changes in surface air temperature is essential to assist decision-making in agriculture and natural resource management. Although there are numerous studies of temperature, temperature data are not always available with adequate resolution or spatial coverage in southern South America. Throughout LPB in particular, data gaps are frequent mainly when weather stations are distant from urban centers. Observations of surface air temperature extremes (minimum and maximum temperature) are sparse, and the quality of chronological records is questionable. Temperature reanalysis helps fill these information gaps and makes it possible to conduct research that would otherwise be unfeasible.

This study has three main purposes: first, to evaluate the distribution of minimum temperature seasonality trends over LPB and describe the trends in the seasonal cycle; second, to identify persistent seasonal changes longer than 10 years; and lastly, to detect changes in minimum temperature extreme events characterized by the number of frost days and the frequency of warm and cold nights. The results are expected to improve the understanding of changes in minimum temperature cycles as drivers of variability in primary production in the basin.

2 Data and methods

2.1 Study area and data

This study focuses on the LPB, which is located in southeastern South America, between 10°S and 36°S and 43°W and 67°W (see Fig. 1). LPB includes part of the territories of five countries: 44% of Brazil, 32% of Argentina, 12% of Paraguay, 7% of Bolivia, and 5% of Uruguay. LPB is one of the most important hydrologic systems in the world, with an area of 3.1 million km^2 that includes a diversity of natural—e.g., forests, grasslands, and shrublands, among others—and agricultural ecosystems.

Given that weather observations in some areas of southeastern South America are scarce and irregularly distributed, datasets providing full spatial coverage are highly valuable for research of this region. Reanalysis databases covering long enough periods for climate analysis are available online and allow real-time updates. The temperature series for this study were retrieved from ECMWF ERA5 reanalysis (European Center for Medium-Range Weather Forecasts; Hersbach et al. 2018). ERA5 is a global high-resolution reanalysis that covers the period between 1979 and the near present. In this study, we use the ERA5 series of daily minimum temperature produced by Chambers (2019) at 0.5° grid resolution in the 1980–2015 period. Furthermore, ERA5, that updates the oldest ERA-Interim version, has been scarcely used in temperature studies in southeastern South America to date. Several studies reported that ERA-Interim was able to reproduce observed trends in seasonal temperature and correctly reproduced the interannual variability of minimum-

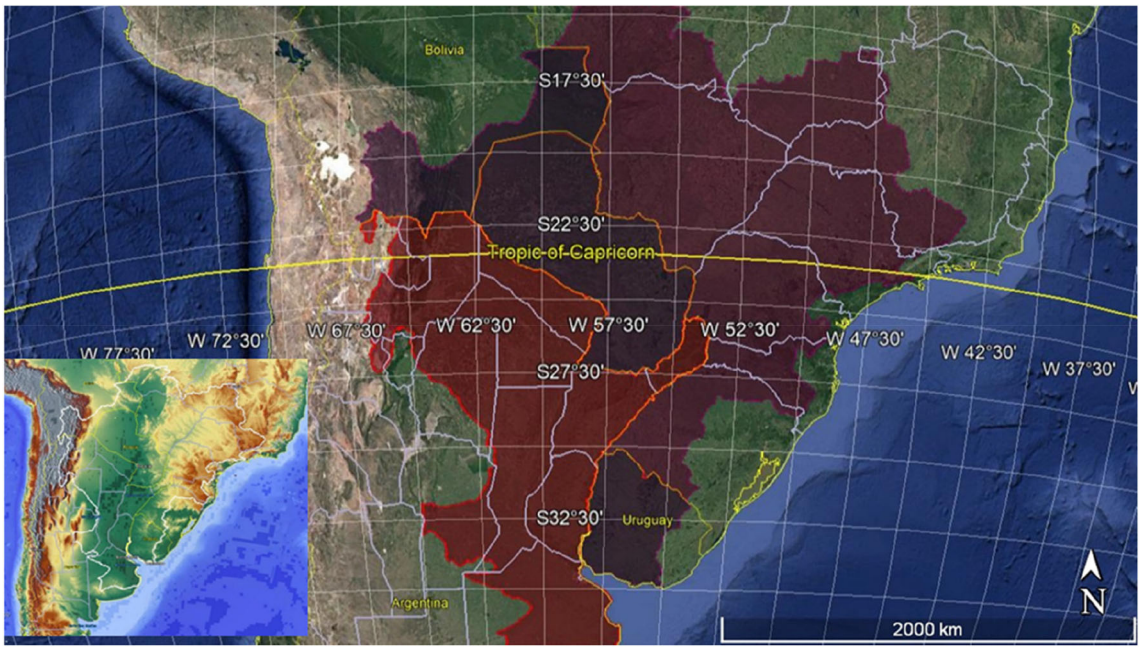

Fig. 1 Map of La Plata river basin (orange line) including country, province, and state borders and southern South America topography (small box—bottom left). Source: Google Earth

temperature extreme events over LPB (e.g., Jones et al. 2012; Cornes and Jones 2013; Lovino et al. 2018b). In contrast, few studies evaluated ERA5 temperature datasets or studied temperature trends. For example, Avila-Diaz et al. (2020) showed that ERA5 could properly recognize observed climate patterns and trends of minimum temperature extremes represented by cold days and cold night indices (TN10p and TN90p, respectively) in the Brazilian part of LPB. These indices presented a small cold bias (almost 5%), very good Pearson correlation coefficients (mainly between 0.8 and 0.9), and small values of RMSE-observations standard deviation ratio (RSR close to 0.5). These results demonstrate the ability of ERA5 to reproduce extreme events related to minimum temperature in this study region. To further test the ERA5 database, this study performed its temperature analysis in the LPB region using the most recent database.

2.2 Methods

2.2.1 Seasonal trend analysis of minimum temperature

Monthly minimum temperature (TnMin) is analyzed by means of extreme temperature indices and seasonal trend analysis. Interannual temperature trends are examined using the seasonal trend analysis (STA; Eastman et al. 2009, 2013). The STA identifies trends in the essential character of the seasonal cycle. It provides an approach to local and regional climate change, filtering out unwanted sources of variability—e.g., sub-annual high-frequency variability and short-term variability. STA specifically rejects high-frequency sub-annual noise and is robust to short-term interannual variability up to a period of 29% of the length of the series; it is able to detect interannual cycles persisting 10 years or more and disregards short-term climate variability (Eastman et al. 2009). Another advantage of STA for trend evaluation of environmental variables is that it provides information on the time of the year when changes occur (Eastman et al. 2009; Neeti and Eastman 2011).

The STA is based on a two-stage time series analysis. The first stage is similar to a Windowed Fourier Analysis. It consists in running a harmonic regression for each year of information to extract the amplitude and phase of sinusoids with annual and semi-annual frequency along with the mean annual temperature. Unlike other trend analysis methods, trends are not calculated over the entire period. Thus, Neeti and Eastman (2011) speak of trends in seasonality. The STA applies harmonic analysis at each grid point to determine the annual average, and annual and semi-annual cycles and the seasonal cycle, as represented by Eq. (1):

$$y = \alpha_0 + \sum_{n=1}^{n=2} \alpha_n \sin\left(\frac{2\pi nt}{T} + \varphi_n\right) \quad (1)$$

where t is the time, T is the period, n is the harmonic, αn are amplitudes, and φn are phase angles (from 0 to 360°).

This way, the seasonality of minimum temperature at each grid point can be expressed by means of five parameters: the annual average amplitude (A0), the amplitude and phase of the annual cycle (A1, F1, respectively), and the amplitude and phase of the semi-annual cycle (A2, F2, respectively). The phase angle (F1) indicates shifts in time, where a value of

30° corresponds to 1 month approximately. The semi-annual cycle is a shape modifier of the annual curve (Eastman et al. 2009). Results depend on the number of harmonics selected, the size of the sample, and the amount of noise in the series.

The second stage calculates a Theil-Sen estimator (TSE, Neeti and Eastman 2011) over time at each pixel for the time series of each shape parameter. TSE calculates the slope for each pairwise combination of samples in time. The median of slopes is then used to characterize the trend, resulting in separate trend maps for each of the five shape parameters over all pixels (Eastman et al. 2009). The statistical significance of the calculated trends is evaluated using the non-parametric Contextual Mann Kendall test (CMK, Neeti and Eastman 2011). The CMK is a robust modification of the Mann Kendall test (MK), which is frequently used for trend analysis of climatic and hydrologic time series (e.g., Yue and Wang 2000; Mavromatis and Stathis 2010). The CMK does not require data to have normal distribution, and it has low sensitivity to abrupt changes due to inhomogeneities in the series (Tabari and Hosseinzadeh Talaee 2011). When comparing CMK and MK results, Ordinola et al. (2017) found insignificant differences in the areas with trends. However, they noted that CMK results were more consistent geographically. This contextual test makes it possible to identify geographical phenomena using spatial autocorrelation, according to which a grid point would be expected to exhibit rather similar trends to those of neighboring grid points.

The statistical significance of the trends in the amplitudes (A0, A1, A2) and the phases of the annual and semi-annual cycles (F1, F2) is evaluated including standardized levels of confidence (Z) and trend directions. The levels of confidence used are as proposed in Neeti and Eastman (2011) ($Z = \pm 2.58$; $Z = \pm 1.96$ and $Z = \pm 1.64$), which correspond to three probability values ($p < 0.1$, 0.05, and 0.01, respectively).

The changes in seasonal behavior over time are reflected in the differences between the resulting annual cycles of the median, calculated using the first and the last years of the total period. This analysis also makes it possible to recognize the time of occurrence of these differences in phase.

2.2.2 Number of frost days and cold and warm nights

Minimum temperature extremes are critical for agriculture in LPB. We use three of the ETCCDI[1] indices (Klein Tank et al. 2009; Zhang et al. 2011) that characterize the frequency of minimum temperature extreme events: the number of frost days (FD), cold nights (TN10p), and warm nights (TN90p). FD is defined as the annual number of days when $TN_{ij} < 0$ °C. TN10p and TN90p are defined as the percentage of days in the year when $TN_{ij} < TN_{in}10$ and $TN_{ij} > TN_{in}90$, respectively. TN_{ij} is daily minimum temperature on day *i* in year j. $TN_{in}90$ or $TN_{in}10$ are 90th or 10th percentile of daily minimum temperature calculated for a 5-day window centered on each calendar day *n* in the base period 1981–2010 (in agreement with Zhang et al. 2011 and Skansi et al. 2013).

We evaluate the spatial distribution of trends in the studied minimum temperature indices in the 1980–2015 period. Trends are computed with the Theil-Sen Method, and statistical significance is determined using the non-parametric Contextual Mann Kendall (both methods are detailed in Section 2.2.1). Areally averaged time series of each index are calculated. We examined the temporal evolution of mean changes in areally averaged minimum temperature indices by fitting polynomial nonlinear trends to each time series.

3 Results and discussion

3.1 Seasonal trends in minimum temperature

Figure 2 presents the spatial distribution of statistically significant trends in annual average amplitude (A0), the amplitudes of the annual (A1) and semi-annual cycles (A2), and the phases of the annual (F1) and semi-annual cycles (F2) of the two variables examined: minimum annual temperature (TnMin) and average minimum temperature (TnMean). Complementarily, a summary of LPB areas with significant trends is presented in Table 1.

Most temperature trends are positive over LPB, as shown in Fig. 2. This warming is revealed by mostly positive changes in A0, A2, and the F1 of both TnMin and TnMean (Fig. 2 a, c, d, f, h, and i). Annual average amplitude (A0) values of TnMin and TnMean exhibit significant changes over 53.5% and 69.9% of LPB, respectively (see Table 1). Figure 2 a and f show that positive changes occur toward the north and east-northeast of LPB, but no significant trends appear in the Humid Pampa. These results agree partially with the results in Zazulie and Rusticucci (2009) who reported that the north and the northeast of LPB present significant trends in the variance explained by the annual cycle of minimum temperature, due to changes in the length of seasons. Significant positive trends in A0 also appear along the Atlantic coast and in the Parana River Delta. Significant negative trends in A0 appear only in TnMin over a small area in the southern extreme of LPB (only 0.3%). Amplitude A1 of TnMin (Fig. 2b) presents significant negative changes over a small area of the basin near Sao Paulo (Brazil) (0.3%, see Table 1). A2 of TnMin (Fig. 2c) exhibits significant positive trends in western Paraguay and northwestern Argentina. The presence of non-zero semi-annual amplitude could be associated either to the existence of a semi-annual cycle in the seasonal curve or to differences in the shape of the annual curve. The F1 of TnMin

[1] World Meteorological Organization (WMO) Commission for Climatology (CCl)/CLIVAR/ JCOMM Expert Team on Climate Change Detection and Indices (ETCCDI)

Table 1 Percentage of La Plata river basin area with significant trends in mean annual amplitude (A0), annual cycle amplitude (A1), semi-annual cycle amplitude (A2), annual cycle phase (F1), and semi-annual cycle phase (F2) of absolute minimum temperature (TnMin) and minimum average temperature (TnMean) for the period 1980–2015

	Area (%) TnMin					Area (%) TnMean				
Significance	A0	A1	A2	F1	F2	A0	A1	A2	F1	F2
NS	46.5	99.7	85.8	89.7	93.9	30.1	98.3	97.2	16.8	99.3
S	53.5	0.3	14.3	10.3	6.1	69.9	1.7	2.8	83.2	0.8
S+	53.2	0.0	12.2	10.3	1.6	69.9	0.0	2.5	83.2	0.6
S-	0.3	0.3	2.1	0.0	4.9	0.0	1.7	0.3	0.0	0.1
S+90	15.3	0.0	3.8	6.4	1.4	11.3	0.0	2.4	19.1	0.6
S+95	12.5	0.0	4.9	3.8	0.2	18.9	0.0	0.1	40.6	0.0
S+99	16.4	0.0	3.5	0.0	0.0	39.7	0.0	0.0	23.4	0.0
S-90	0.2	0.3	1.2	0.0	4.5	0.0	1.7	0.3	0.0	0.1
S-95	0.1	0.0	0.7	0.0	0.4	0.0	0.0	0.0	0.0	0.0
S-99	0.0	0.0	0.2	0.0	0.0	0.0	0.0	0.0	0.0	0.0

Significant (S±) or non-significant (NS±) trends; sign indicates positive/negative trends; and 90, 95, and 99 indicate confidence levels

(Fig. 2d) shows significant lags in the northern part of the basin. Positive trends are indicative of anticipated occurrence of maximum TnMin in the 1980–2015 period, suggesting that the warm season tends to begin earlier in the year.

Amplitudes and phases of TnMean are presented in Fig. 2 f–j. Figure 2f shows that the areas with significant trends in the amplitude of TnMean present some similitudes in coverage with those of TnMin (Fig. 2a). The annual cycle amplitude A1 presents significant negative trends in small portions of LPB (1.7%, Fig. 2g), a bit more than the 0.3% detected in TnMin, although these significant negative trends are not congruent in location. The presence of a trend in the semi-annual pattern of A1 does not necessarily imply a trend in the seasonal cycle; it is rather an indication of a change in the shape of the annual curve. Neither TnMin nor TnMean presents significant positive trends of A1 in LPB. The A2 of TnMean (Fig. 2h) exhibits significant increases in a small area in the northwest of LPB (2.5%). Nevertheless, the phase of the annual cycle F1 of TnMean presents a significant positive trend in almost the entire basin (83.2%). The trend mostly concentrates in the center and northeast of LPB (Fig. 2i and Table 1).

The amplitudes of the semi-annual cycle of absolute and average minimum temperatures have non-significant trends over more than 85% of LPB (Table 1). Spatial patterns of the phase of absolute minimum temperatures present non-significant trends in more than 89.7% of LPB, but spatial patterns of the phase of average minimum temperatures are significant in 83.2% of LPB (see Table 1 and Fig. 2 d and i).

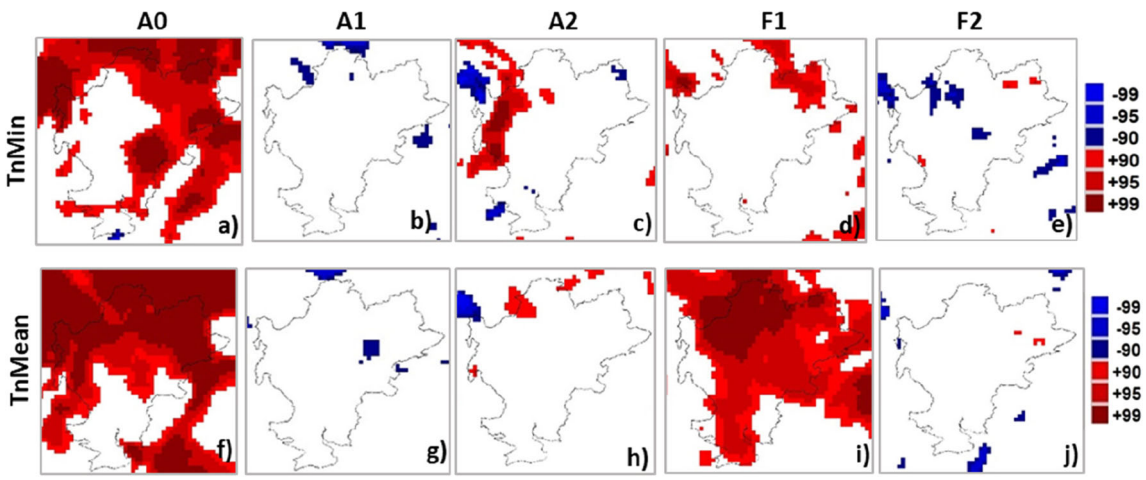

Fig. 2 Areas in La Plata basin with statistically significant trends (1980–2015) (ERA5 database) of mean annual amplitude (A0), annual cycle amplitude (A1), semi-annual cycle amplitude (A2), phase of the annual cycle (F1), and phase of semi-annual cycle (F2) of absolute minimum temperature (TnMin **a**, **b**, **c**, **d**, **e**) and average minimum temperature (TnMean, **f**, **g**, **h**, **i**, **j**). Warm colors (red) indicate significant positive trends, while cold colors (blue) highlight significant negative trends. Significance confidence levels are 90%, 95%, and 99%

The analysis of the average minimum temperature (TnMean) reveals that relevant changes include an earlier occurrence of the maximum shift in phase (F1) indicative of anticipated occurrence of minimum temperature. The phases of the annual cycles of TnMin and TnMean present positive trends in the north and northeast of LPB. Persistent changes are observed over a significant area, in agreement with Victoria et al. (1998) and Rosso et al. (2015).

Significant monotonic trends in TnMin and TnMean only appear in northeastern Argentina. Given that cloud cover could affect these variables, the conclusions in Barrucand and Rusticucci (2001) and Barrucand (2008) could provide some support to our results, as those authors found that the cloud cover remains unchanged along the diurnal cycle in northeastern Argentina. Zazulie and Rusticucci (2009) obtained similar results and observed an area without trends in the variance explained by the amplitude of the annual cycle of TnMin, TnMean, and TnMax in the 1961–2003 period. They found negative trends in the annual cycle of TnMax. On the contrary, trends were mainly positive when considering TnMin. Furthermore, Collazo et al. (2019a) noted a decrease in the frequency of cold extremes, which is consistent with the existence of positive trends in TnMin and TnMean identified in our study.

Figures 3 present the areas where significant trends in A0 (Fig. 3a) and F1 (Fig. 3b) of both the TnMin and TnMean overlap. Figure 3a shows a match in the areas with significant trends of the mean amplitudes of both variables in the northeast of the basin. Moreover, such trends are positive in both variables. Figure 3b shows that F1 also presents positive trends for both TnMin and TnMean toward northeastern LPB. The phase of the annual cycle of TnMin (F1, Fig. 2d) presents positive significant trends up to 0.39 days in the northeast of LPB in the 1980–2015 period. Furthermore, TnMean presents positive trends up to 0.36 days in 36 years in almost entire LPB (see Fig. 2i), with average trend of 0.1 ± 0.08 days. The trends in F1 for TnMean are less pronounced than those found in Stine et al. (2009), who indicated that the phase of the annual cycle of surface temperature over extratropical land shifted toward earlier seasons by 1.7 days between 1954 and 2007, which they interpreted as being indicative of a natural oscillation.

Figure 4 presents the trends in TnMin and TnMean in the 1980–2015 period together with the trends in A0. The spatial patterns and magnitudes of trends of both TnMin and TnMean and their average amplitudes are quite similar (compare Fig. 4a with Fig. 4 c and b with d). Significant trends in the mean amplitude A0 of both variables (Fig. 2 a and f) are in general agreement with TnMin and TnMean significant trends (not shown), presenting overlapped significant positive trends in the northern area of LPB.

Significance levels of the correlation coefficients are high (r^2 = 0.96), as calculated with the Theil Sen method. Considering only the grid points with statistically significant trends, and relating them to gradient values (i.e., the rate of change of average TnMin at those grid points), the trends reach + 0.035 °C/year and + 0.025 °C/year. Total variation throughout the period is + 1.26 °C and + 0.9 °C in TnMin and TnMean, respectively. This warming is consistent with the results of Falvey and Garreaud (2009), Skansi et al. (2013), Lovino et al. (2018b), and Collazo et al. (2019a, b), among others.

Figure 5 presents the regression analysis between trends in TnMin and TnMean and trends in A0 for the same variables in the entire LPB in the 1980–2015 period. Both variables present a correlation of 0.98 and more than 96.0% of variance explained by the linear trend. These results suggest that a large proportion of the variance in A0 calculated for TnMin and TnMean can be explained by a linear trend (see Fig. 5). The correlation between the trends of TnMean and TnMin was rated using CMK coefficients. Correlations of A0 and F1 (not shown) between the series of TnMean and TnMin reached a determination coefficient (r^2) of 0.65 and 0.29, respectively, reinforcing the idea that both series have more in common in terms of their average values than in terms of the annual phase.

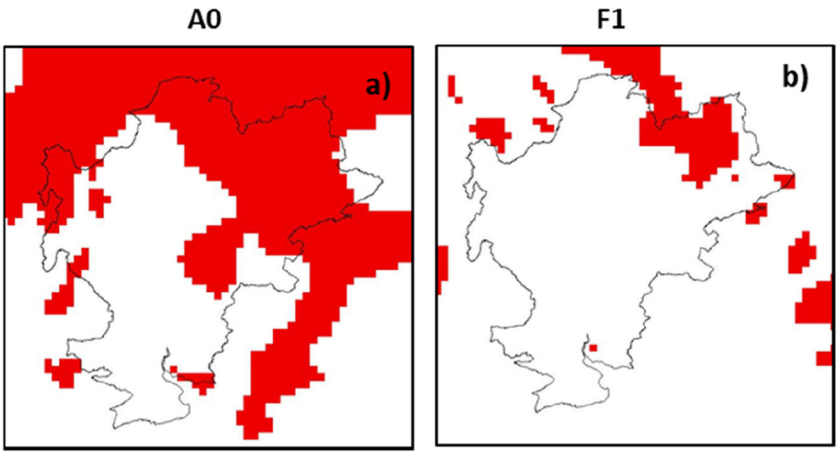

Fig. 3 Regions where significant trends in absolute minimum temperature (TnMin) and average minimum temperature (TnMean) overlap for each parameter: mean annual amplitude (A0) in panel (**a**) and the phase of the annual cycle (F1) in panel (**b**). Red color indicates that TnMin and TnMean have positive trends overlapped (+). There are no other combinations in LPB

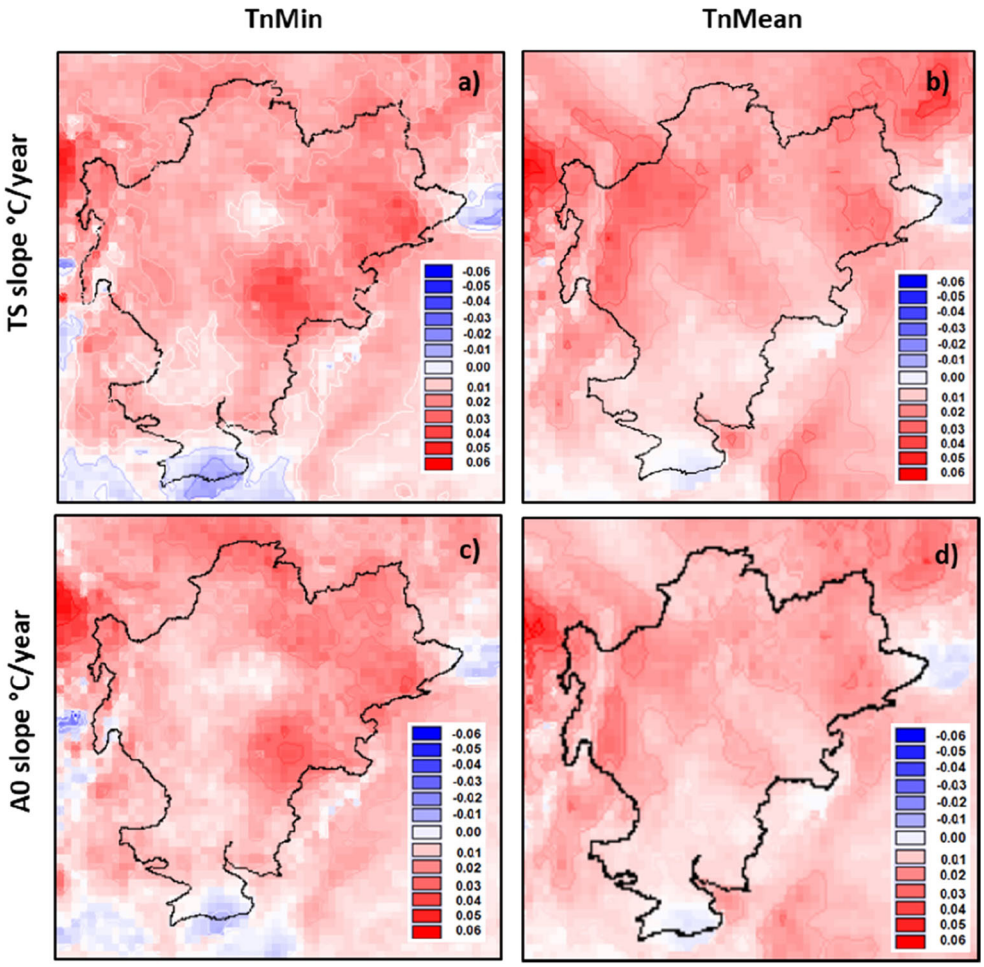

Fig. 4 Theil Sen trend (TS, °C/year) for (**a**) absolute minimum temperature (TnMin) and (**b**) average minimum temperature (TnMean) over La Plata river basin (1980–2015). Linear trend (°C/year) for average amplitude of (**c**) TnMin (A0 TnMean) and (**d**) average amplitude of TnMin (A0 TnMean, °C/year)

Figure 6 presents the combination of amplitudes (A0 in red, A1 in green, and A2 in blue), and Fig. 7 presents combination of phases (A0 in red, F1 in green, and F2 in blue). Color combinations indicate parameters with greater positive trends. For example, bright magenta indicates positive trends in both A0 and A2. In order to analyze and interpret the characteristics of the annual cycles, some locations were studied in detail, comparing reanalysis, observations, and fitted curves. Figures 6 and 7 show the annual cycles of TnMin and TnMean based on the ERA5 dataset, weather station

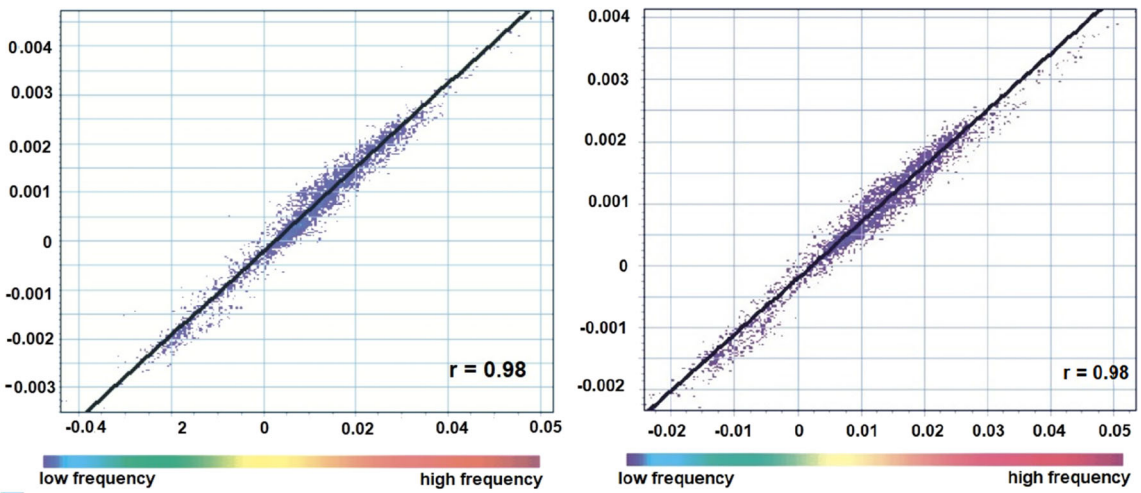

Fig. 5 Regression analysis between the mean annual amplitude A0 Theil Sen slope and the linear trend for absolute minimum temperature (TnMin, left) and average minimum temperature (TnMean, right) over La Plata river basin (1980–2015)

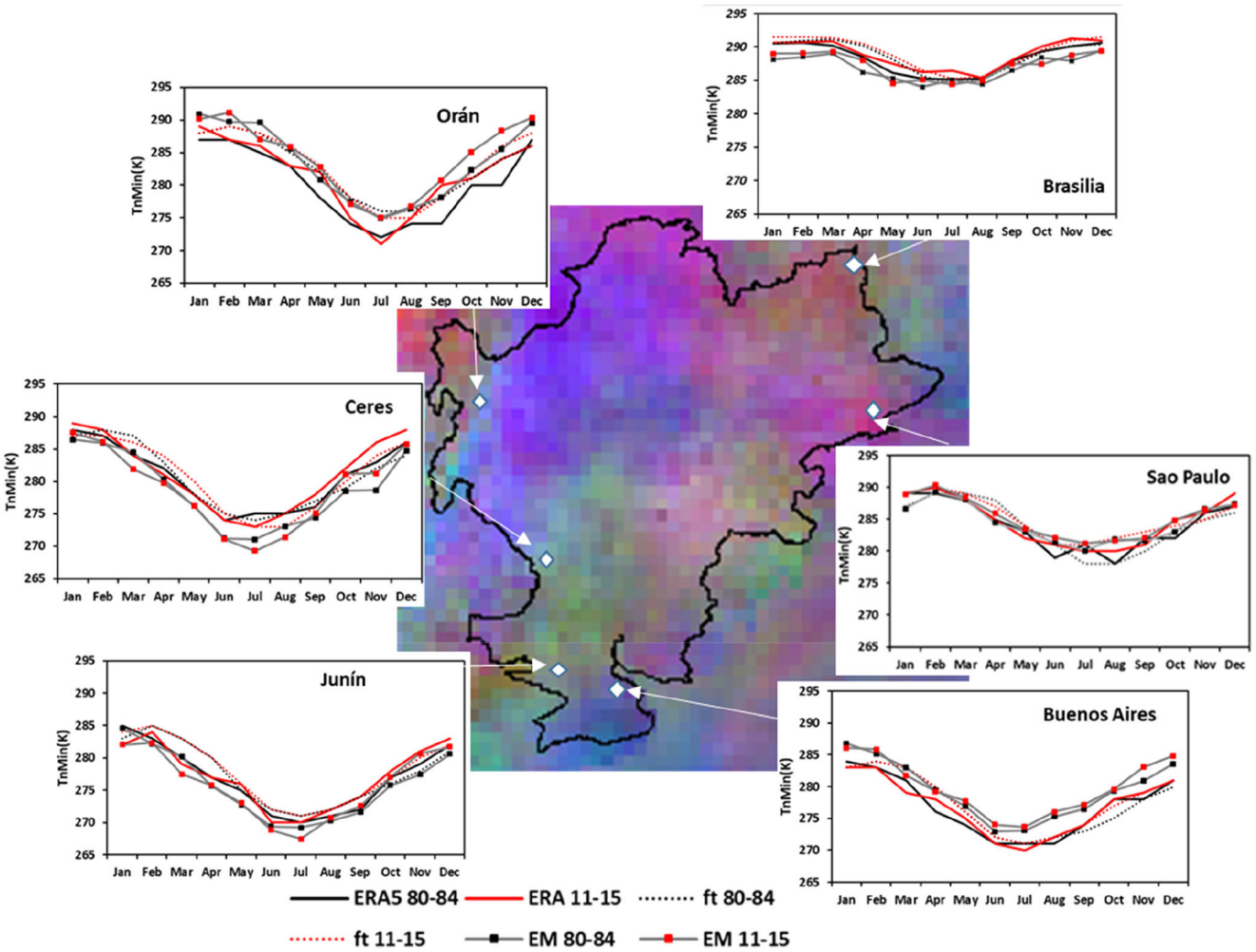

Fig. 6 Selected locations with data from weather stations (EM 80-84 and EM 11-15), ERA5 (ERA5 80-84 and ERA5 11-15), and fitted (ft 80-84 and ERA5 11-15) absolute minimum temperature (TnMin) for 1980–1984 and 2011–2015. The color composite is an RGB combination of the mean annual amplitude (A0 in red), the amplitude of the annual cycle, (A1 in green), and the amplitude of the semi-annual cycle (A2 in blue)

observations, and data fitted by STA, respectively, in the first and last 5-year intervals of the study period (1980–1984; 2011–2015). TnMin rose in Brasilia, Oran, and Ceres (see Fig. 6), mainly in summer, with a warming of up to 3.0 °C toward the end of the period under study.

On the other hand, warmer TnMin is observed in different seasons, depending on the area. Near the Andes (Oran, Fig. 6), temperature rises in spring and early summer, while in Brasilia (Fig. 6), it rises between 2.0 and 3.0 °C in summer and autumn. At the remaining stations (Junín and Sao Paulo, Fig. 6), absolute minimum temperature rose about 1.0 °C almost throughout the whole year in the study period. Close to the Atlantic Ocean coast, significant warming occurred in all seasons but on a smaller scale than in the rest of the analyzed subareas. These results agree with the increase in the amplitude of the semi-annual amplitude A2 of TnMin, as an amplification of the annual curve amplitude. The phase shows a shift in the annual TnMin wave at some statistically significant grid points located mainly in the northern area of La Plata river basin. Figure 7 shows that TnMean increased in Brasilia, Oran, and Ceres (see Fig. 7) mainly from winter to summer. Most locations underwent a phase shift (Fig. 7) that could be easily observed in the fitted curves.

3.2 Trends in frost days and cold and warm nights

Figure 8 presents the spatial distribution of the linear trends of FD, TN10p, and TN90p and their statistical significance as well as the areally averaged time series. No remarkable trends are observed in FD in most of LPB. The Andes, in the western corner of the LPB, are an exception, since the number of frost days has decreased significantly (with a maximum decay rate of one frost day per year) in the period under study (Fig. 8 a and b). The highest areas of the LPB, i.e., its Andean portion, had more than 300 FD per year. On the other hand, the frequency of frost days in the Chaco-Pampa plain varies latitudinally, from 30 frost days per year in the south of LPB to no frost days in the north (not shown). No significant trends are

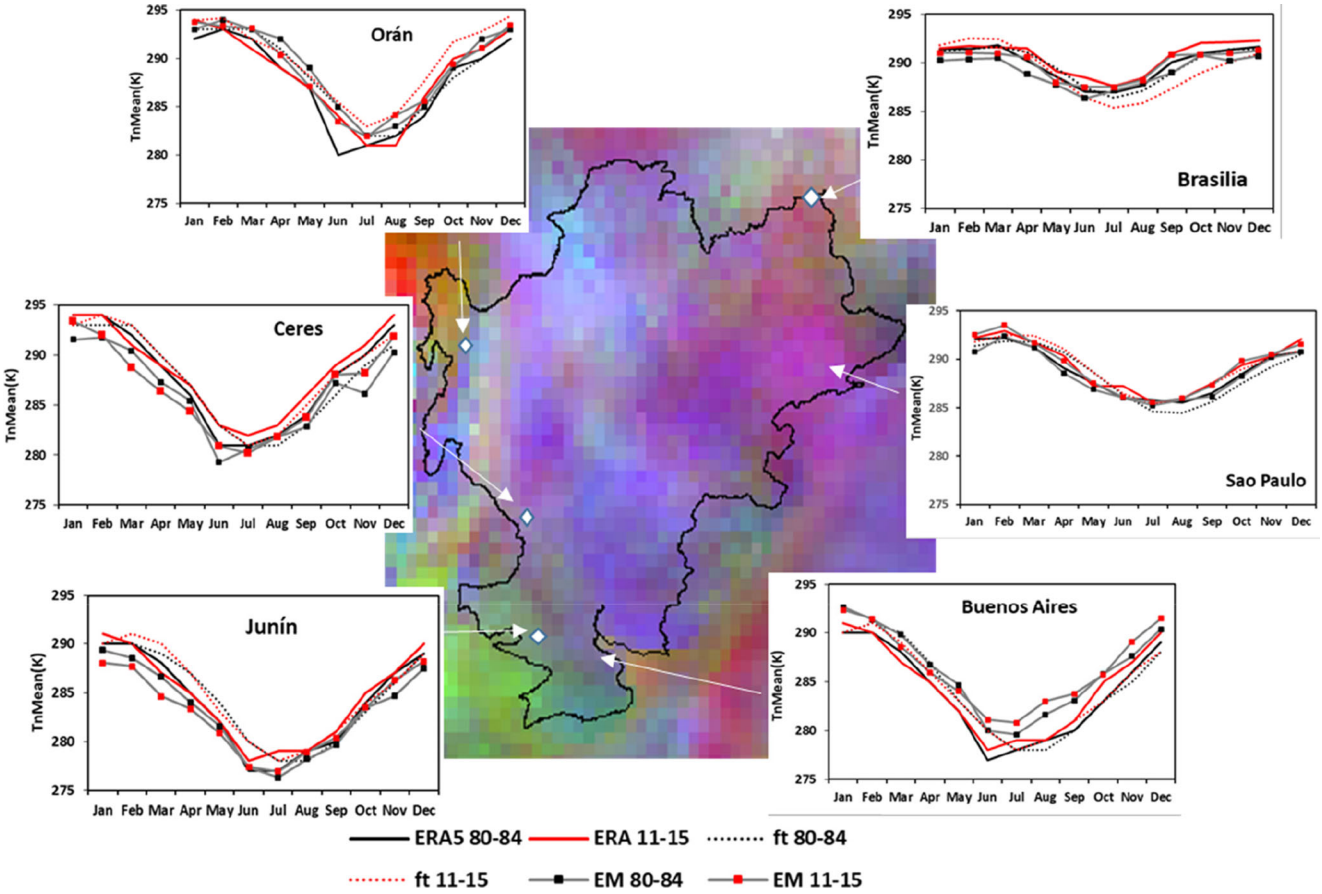

Fig. 7 Selected locations with data from weather stations (EM 80-84 and EM 11-15), ERA5 (ERA5 80-84 and ERA5 11-15), and fitted (ft 80-84 and ERA5 11-15) mean minimum temperature (TnMean) for 1980–1984 and 2011–2015. The area color composite is an RGB combination of the mean annual amplitude (A0 in red), the phase of the annual cycle (F1 in green), and the phase of the semi-annual cycle (F2 in blue)

found in the large LPB plain, where extensive agro-industrial activities take place. Thus, areally averaged time series of FD over the whole LPB (Fig. 8c) show a slight decrease in the number of frost days, since the area with significant changes is small compared to the total size of the basin.

The frequency of warm nights exhibits a significant increase in most of LPB, particularly toward the north (Fig. 8 d and e). The greatest increase occurred in the northeastern corner of LPB, where TN10p grew at a rate of 0.35% days per year. The significance of increases of warm nights toward the north is at 95% level (Fig. 8e). The areally averaged frequency of warm nights (Fig. 8f) reveals an increase from 8 to 13% days per year from about 1990 to 2015 with important interannual variability. Interestingly, the areally averaged mean trend of cold nights (Fig. 8i) shows that the frequency of cold nights decreased by about 3% from 1990 to 2015, that is, at the same time when an increase of about 5% was observed in the frequency of warm nights (Fig. 8f). Decreasing cold night frequency was observed in the whole LPB (Fig. 8g), with significant trends at least at the 99% confidence level in the north and northwestern LPB (Fig. 8h). The highest decrease rates of cold nights reach values of 0.3% days per year, in the northeast of LPB (Fig. 8g).

4 Conclusions

This paper analyzes seasonal trends in absolute minimum temperature (TnMin), average minimum temperature (TnMean), and in the frequency of cold days (TN10p), warm nights (TN90p), and frost days (FD) computed using ERA5 reanalysis over La Plata river basin in the period 1980–2015. Minimum temperature over LPB presented trends in the seasonal cycle as well as variations and trends described in terms of the annual and semi-annual amplitudes and phases. Both amplitude and phase parameters suggested that average minimum temperature underwent greater variation than absolute minimum temperature over LPB.

The seasonal trend analysis made it possible to identify trends in the seasonality of minimum absolute temperature. In general, the annual cycles of mean and absolute minimum temperature—TnMean and TnMin, respectively—were

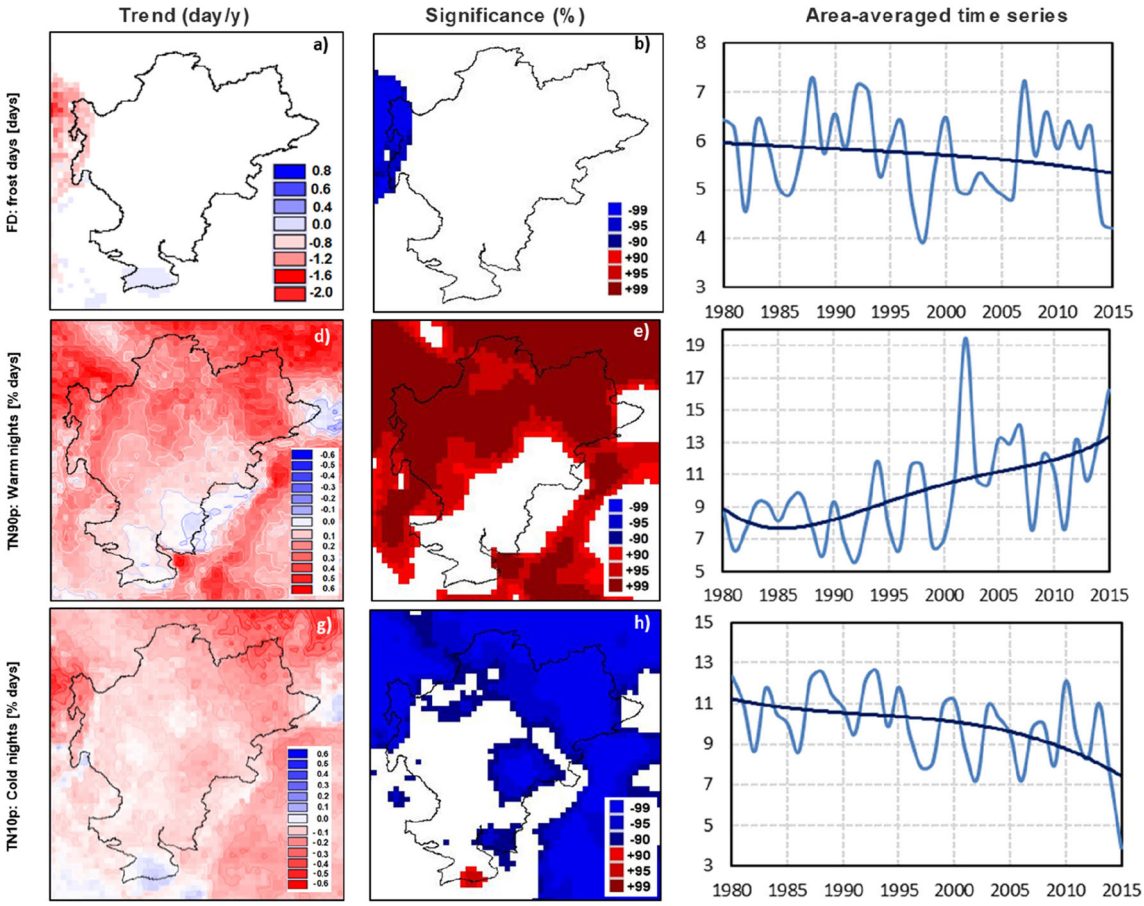

Fig. 8 Number of frost days (FD, first row), warm nights (TN90p, second row), and cold nights (TN10p, third row). Left panels (**a**, **d**, **g**): trends computed with the Theil Sen Method (°C/year) for the 1980–2015 period. Middle panels (**b**, **e**, **h**): areas with statistically significant trends. Significance scale is presented at the bottom of the column. Right panels (**c**, **f**, **i**): temporal evolution of areally averaged indices over LPB and their nonlinear trends estimated by fitting polynomial trends

positive throughout LPB in the period 1980–2015. Heterogenous spatial patterns of significant changes were found for the amplitude of the annual average (A0) and the amplitude and phase of the annual cycle (A1 and F1) for both TnMean and TnMin. The most important changes were observed in the annual average amplitude (A0) (in 53.5% and 69.9% of the area, respectively) and in the phase of the annual cycle, F1 (10.3% and 83.2%, respectively) of both variables—TnMean and TnMin. The significant trend observed in phase F1 implies a shift toward warmer seasons. This shift was less than that reported in the northern hemisphere by Stine et al. (2009). The area average of F1 presented an increase of 16.3°, which corresponds to a shift of approximately 16 days toward warmer seasons.

The amplitude of the annual cycle (A1) showed almost no significant trends for both TnMin and in TnMean over LPB. On the other hand, the phase of the annual cycle (F1) showed greater differences in the spatial coverage of positive trends between TnMin and TnMean. The only region in which the positive trends of F1 coincided was toward the north of LPB. These results reinforced the idea that both series (TnMin and TnMean) have more in common in terms of their average values, as demonstrated by the trends in A0, than in terms of the angle/timing of the annual phase. However, a significant increase was reported for the A0 in TnMin in more than half of the basin (53.5% of the LPB), while significant changes if F1 for TnMean for more than 80% of the LPB revealed a prevailing shift to anticipate the occurrence of its maximum. Stine et al. (2009) suggested that the phase shift is related with several mechanisms but highly influenced by changes in thermal mass. Thermal mass on land is largely modulated by soil moisture. If soil moisture decreases, it would result in a positive phase shift. A significant negative trend of soil moisture in a great percentage of LPB from 1979 to 2017 was reported by Deng et al. (2020). This soil moisture decrease would be related with the phase shift to earlier seasons.

The annual average TnMin and TnMean showed a positive trend mainly in the north and the east of LPB. These results are consistent with the findings of Zazulie and Rusticucci (2009) who reported that these areas present significant trends in the

variance explained by the annual cycle of minimum temperature, due to changes in the length of the different seasons. Negative trends in absolute and mean minimum temperature were observed in the south of the basin; however, only TnMin trends were significant. Our results also reported a great percentage of significant positive trends closer to the eastern coast of South America not only for the average amplitude, the amplitude, and phase of the annual cycle but also for the frequency of cold and warm nights. Renom et al. (2011) suggested that minimum temperature extremes over the eastern South American coast are forced by sea surface temperatures in the Atlantic Ocean LPB and internal atmospheric variability. In addition, it is well known that climate in South America underwent a change in the 1970s, which was connected to the 1976–1977 global climate shift (Jacques-Coper and Garreaud 2015). This climate shift appears to have been a source of change in temperature trends and variability. For example, Renom et al. (2011) found that changes in El Niño evolution after 1976 may have altered the relationship between temperature extreme events in the South American coast and atmospheric circulation.

Minimum temperature extremes are becoming warmer throughout LPB. The frequency of warm and cold nights shows significant signals of warming: while the number of warm nights has been increasing since 1990, cold night frequency has been decreasing in the same period. These results agree with those reported for the region by Skansi et al. (2013), Lovino et al. (2018b), and Collazo et al. (2019a, b). Minimum temperature warming may have impacts on agriculture (Barros et al. 2015; Lovino et al. 2018a). The rise in average minimum temperature together with decreasing number of cold nights led to increased evapotranspiration rates in wheat and barley and shortening of grain-filling periods, which resulted in a drop in yields (Magrin et al. 2009; García et al. 2015; Hatfield and Prueger 2015).

Even the coldest region of LPB, i.e., the highest Andes mountains, saw a significant decrease in the number of frost days. Contrarily, no significant changes were observed in the number of frost days over most of the LPB region, including the Chaco-Pampa plain and the Brazilian plateau. However, El Niño Southern Oscillation—ENSO—is known to favor large interannual variability in frost day frequency over this region: less frost days are observed during El Niño years and more in La Niña years (Müller et al. 2000; Müller et al. 2003; Lovino et al. 2018b).

Greenhouse gas (GHG) emissions and land-use changes are widely accepted as major drivers of climate changes, particularly changes in temperature and precipitation (e.g., Magrin et al. 2014; Allen et al. 2018). Over the past decades, La Plata basin has been subject to major changes in land cover, which in turn are modifying latent and sensible heat and soil moisture in the area (e.g., Lee and Berbery 2012). Avila et al (2012) found that minimum temperature extremes present locally strong and statistically significant responses to induced land cover change over LPB. Our findings revealed that the significant warming of absolute minimum temperatures in central and northern LPB and the weak cooling in the south of the basin are consistent with the results reported by Avila et al (2012) when considering temperature indices related to land use and land cover changes. In LPB, 0.1 to 0.5 of the fraction of vegetation cover was converted from forest to cropland, which means that the scale of the impact is large enough to be significant on seasonal timescales (Avila et al. 2012).

Acknowledgment We are grateful to the anonymous reviewers whose constructive comments and recommendations helped to improve the manuscript.

Authors' contributions All authors contributed to the study conception and design. Material preparation, data collection, and analysis were performed by Marisa Cogliati and Miguel Lovino. The first draft of the manuscript was written by Marisa Cogliati, and all authors commented on previous versions of the manuscript. All authors read and approved the final manuscript.

Funding This work was supported by the Universidad Nacional del Comahue (04-H165).

Data availability ERA5 daily temperature data here used are available at Chambers (2019) ERA5-derived daily temperature summary 1980-2018 (Version 1.0) [Dataset]. Zenodo. doi:10.5281/zenodo.3403963

Compliance with ethical standards

Conflict of interest The authors declare that they have no conflict of interest.

Code availability Not applicable.

References

Alexander L, Zhang X, Peterson T, Caesar J, Gleason B, Klein Tank A (2006) Global observed changes in daily climate extremes of temperature and precipitation. J Geophys Res 111(D5). https://doi.org/10.1029/2005jd006290

Allen MR, de Coninck H, Dube OP et al (2018) Technical Summary. In Masson-Delmotte V, Zhai P, Pörtner H-O, Roberts D et al (eds) Global Warming of 1.5 °C. An IPCC Special Report on the impacts of global warming of 1.5 °C above pre-industrial levels and related global greenhouse gas emission pathways, in the context of strengthening the global response to the threat of climate change, sustainable development, and efforts to eradicate poverty

Arsego DA, Ferraz SET, Nereu AS, Cardoso A, Zanon AJ (2018) Study of the impact of different indices associated with El Niño southern oscillation on soybean yield in Rio Grande do Sul. Ciência e Natura, Santa Maria 40:82–87 https://periodicos.ufsm.br/cienciaenatura/issue/view/1304

Avila FB, Pitman AJ, Donat MG, Alexander LV, Abramowitz G (2012) Climate model simulated changes in temperature extremes due to land cover change, J Geophys Res 117. https://doi.org/10.1029/2011JD016382

Avila-Diaz A, Benezoli V, Justino F, Torres R, Wilson A (2020) Assessing current and future trends of climate extremes across Brazil based on reanalyses and earth system model projections. Clim Dyn 55:1403–1426. https://doi.org/10.1007/s00382-020-05333-z

Barros V, Clarke R, Dias PS (2006) Climate change in the La Plata Basin. Consejo Nacional de Investigaciones Científicas y Técnicas, Buenos Aires. Website: http://www.cicplata.org/

Barros VR, Boninsegna JA, Camilloni IA, Chidiak M, Magrín GO, Rusticucci M (2015) Climate change in Argentina: trends, projections, impacts and adaptation. WIREs Clim Chang 6:151–169. https://doi.org/10.1002/wcc.316

Barrucand M (2008) Extremos de temperatura en Argentina: Cambios observados en la variabilidad espacio-temporal y su relación con otras características del sistema climático. Tesis de Doctorado en Ciencias de la Atmósfera y los Océanos, Universidad de Buenos Aires, pp 162

Barrucand M, Rusticucci M (2001) Climatología de temperaturas extremas en la Argentina. Variabilidad temporal y regional. Meteorol 26:85–101

Berlato MA, Farenzha H, Fontana DC (2005) Associação entre El Niño Oscilação Sul e a produtividade do milho no Estado do Rio Grande do Sul. Pesq Agrop Brasileira 40:423–432

Berri GJ, Bertossa G (2004) The influence of the tropical and subtropical Atlantic and Pacific Oceans on precipitation variability over southern central South America on seasonal time scales. Int J Climatol 24: 415–435

Carril AF, Cavalcanti IFA, Menéndez CG et al (2016) Extreme events in the La Plata basin: a retrospective analysis of what we have learned during CLARIS-LPB project. Clim Res 68:95–116. https://doi.org/10.3354/cr01374

Chambers J (2019) ERA5-derived daily temperature summary 1980-2018 (Version 1.0) [Data set]. Zenodo. https://doi.org/10.5281/zenodo.3403963

Collazo S, Barrucand M, Rusticucci M (2019a) Variability and predictability of winter cold nights in Argentina. Weather Climate Extremes 26:100236. https://doi.org/10.1016/j.wace.2019.100236

Collazo S, Barrucand M, Rusticucci M (2019b) Summer seasonal predictability of warm days in Argentina: statistical model approach. Theor Appl Climatol 138(3-4):1853–1876. https://doi.org/10.1007/s00704-019-02933-6

Comité Intergubernamental Coordinador de los Países de la Cuenca del Plata (CIC) (2017) Transboundary Diagnostic Analysis for the La Plata River Basin - TDA. 1st edition. https://cicplata.org/es/documentosprincipales/?sfw=pass1610131282. Accessed 10 May 2020.

Cornes R, Jones P (2013) How well does the ERA-Interim reanalysis replicate trends in extremes of surface temperature across Europe? J Geophys Res Atmos 118:10262–10276. https://doi.org/10.1002/jgrd.50799

Deng Y, Wang S, Bai X, Luo G, Wu L, Cao Y, Li H, Li C, Yang Y, Hu Z, Tian S (2020) Variation trend of global soil moisture and its cause analysis. Ecol Indic 110:105939. https://doi.org/10.1016/j.ecolind.2019.105939

Eastman JR, Sangermano F, Ghimire B, Zhu H, Chen H, Neeti N (2009) Seasonal trend analysis of image time series. Int J Remote Sens 30(10):2721–2726. https://doi.org/10.1080/01431160902755338

Eastman JR, Sangermano F, Machado EA, Rogan J, Anyamba A (2013) Global trends in seasonality of NDVI, 1982-2011. Remote Sens 5(10):4799–4818. https://doi.org/10.3390/rs5104799

Falvey M, Garreaud RD (2009) Regional cooling in a warming world: recent temperature trends in the southeast Pacific and along the west coast of subtropical South America (1979–2006). J Geophys Res 114:D04102. https://doi.org/10.1029/2008JD010519

Fernández Long ME, Müller GV, Beltrán-Przekurat A, Scarpati OE (2013) Long-term and recent changes in temperature-based agroclimatic indices in Argentina. Int J Climatol 33(7):1.673–1.686

García GA, Dreccer MF, Miralles DJ, Serrago RA (2015) High night temperatures during grain number determination reduce wheat and barley grain yield: a field study. Glob Chang Biol 21:4153–4164

García GA, Serrago RA, Dreccer MF, Miralles DJ (2016) Post-anthesis warm nights reduce grain weight in field-grown wheat and barley. Field Crop Res 195:50–59

Hatfield JL, Prueger JH (2011) Agroecology: implications for plant response to climate change. Book Editor(s): Yadav SS, Redden RR, Hatfield JL, Lotze-Campen H, Hall AE https://doi.org/10.1002/9780470960929

Hatfield JL, Prueger JH (2015) Temperature extremes: effect on plant growth and development. Weather Climate Extremes 10(A):4–10. https://doi.org/10.1016/j.wace.2015.08.001

Hersbach H, Rosnay P, Bell B et al (2018) Operational global reanalysis: progress, future directions and synergies with NWP. In: ECMWF Report, p 65. https://www.ecmwf.int/node/18765

Jacques-Coper M, Garreaud RD (2015) Characterization of the 1970s climate shift in South America. Int J Climatol 35:2164–2179. https://doi.org/10.1002/joc.4120

Jones P, Lister D, Osborn T, Harpham C, Salmon M, Morice C (2012) Hemispheric and large-scale land-surface air temperature variations: an extensive revision and an update to 2010. J Geophys Res Atmos 117(D5):n/a-n/a. https://doi.org/10.1029/2011jd017139

Klein Tank AMG, Zwiers FW, Zhang X (2009) Guidelines on analysis of extremes in a changing climate in support of informed decisions for adaptation, WMO-TD No. 1500/WCDMP-No. 72, Geneva. (52 pp.)

Lee SJ, Berbery EH (2012) Land cover change effects on the climate of the La Plata Basin. J Hydrometeorol 13:84–102

Lovino MA, Müller OV, Müller GV, Sgroi LC, Baethgen WE (2018a) Interannual-to-multidecadal hydroclimate variability and its sectoral impacts in northern Argentina. Hydrol Earth Syst Sci 22:3155–3174. https://doi.org/10.5194/hess-22-3155-2018

Lovino MA, Müller O, Berbery EH, Müller G (2018b) How have daily climate extremes changed in the recent past over northeastern Argentina? Glob Planet Chang 168:78–97. https://doi.org/10.1016/j.gloplacha.2018.06.008

Magrin GO, Travasso MI, Rodriguez GR, Solman S, Nuñez M (2009) Climate change and wheat production in Argentina. Int J Glob Warming 1(1/2/3):214–226. https://doi.org/10.1504/IJGW.2009.027090

Magrin GO, Marengo JA, Boulanger J-P et al (2014) Central and South America. In: Barros VR, Field CB, Dokken DJ et al (eds) Climate Change 2014: Impacts, Adaptation, and Vulnerability. Part B: Regional Aspects. Contribution of Working Group II to the Fifth Assessment Report of the Intergovernmental Panel on Climate Change. Cambridge University Press, Cambridge, United Kingdom and New York, NY, USA, pp 1499–1566

Mavromatis T, Stathis D (2010) Response of the water balance in Greece to temperature and precipitation trends. Theor Appl Climatol 104(1-2):13–24. https://doi.org/10.1007/s00704-010-0320-9

Mayeregger E, Casco M, Vera A (2015) "El Niño" y sus Impactos en el Sector Agrícola del Paraguay. Revista sobre Estudios e Investigaciones del Saber Académico. 9. http://publicaciones.uni.edu.py/index.php/eisa/article/view/97

Müller G, Nuñez M, Seluchi M (2000) Relationship between ENSO cycles and frost events within the pampa Húmeda region. Int J Climatol 20:1619–1637. https://doi.org/10.1002/1097-0088(20001115)20:13<1619::AID-JOC552>3.0.CO;2-F

Müller GV, Compagnucci R, Nuñez M, Salles A (2003) Surface circulation associated with frosts in the wet pampas. Int J Climatol 23(8): 943–961. https://doi.org/10.1002/joc.907

Müller GV, Fernández Long ME, Bosch E (2011) Relación entre la temperatura de la superficie del mar de diferentes océanos y los

rendimientos del maíz en la pampa húmeda. Meteorológica 40(1):5–16

Neeti N, Eastman JR (2011) A contextual Mann-Kendall approach for the assessment of trend significance in image time series. Trans GIS 15(5):599–611

Ordinola RN, Cogliati MG, Müller G (2017) Evaluación de la tendencia de la temperatura mínima en la cuenca del Plata entre 1980-2015 utilizando datos de reanálisis. In XXVIII Reunión Científica de la AAGG. La Plata. Retrieved from http://hdl.handle.net/10915/60718

Penalba OC, Bettolli ML, Vargas WM (2007) The impact of climate variability on soybean yields in Argentina. Multivariate regression. Meteorol Appl 14:3–14

Piñeiro G, Oesterheld M, Paruelo JM (2006) Seasonal variation in aboveground production and radiation-use efficiency of temperate rangelands estimated through remote sensing. Ecosystems 9(3): 357–373

Renom M, Rusticucci M, Barreiro M (2011) Multidecadal changes in the relationship between extreme temperature events in Uruguay and the general atmospheric circulation. Clim Dyn 37:2471–2480. https://doi.org/10.1007/s00382-010-0986-9

Rosso FV, Boiaski NT, Ferraz SET, Dewes CF, Tatsch JD (2015) Trends and decadal variability in air temperature over Southern Brazil. Am J Environ Eng 5(1A):85–95. https://doi.org/10.5923/s.ajee.201501.12

Sadras V, Monzón J (2006) Modelled wheat phenology captures rising temperature trends: Shortened time to flowering and maturity in Australia and Argentina. Field Crop Res 99:136–146

Skansi MM, Brunet M, Sigró J, Aguilar E, Arevalo Groening JA, Betancour OJ, Castellón Geier YR, Correa Amaya RL, Jácome H, Malherios Ramos A, Oria Rojas C, Pasten A, Sallons Mitro S, Villaroel C, Martínez R, Alexander LV, Jones PD (2013) Warming and wetting signals emerging from analysis of changes in climate extreme indices over South America. Glob Planet Chang 100:295–307. https://doi.org/10.1016/j.gloplacha.2012.11.004

Stine AR, Huybers PJ, Fung IY (2009) Changes in the phase of the annual cycle of surface temperature. Nature 457:435–440

Tabari H, Hosseinzadeh Talaee P (2011) Analysis of trends in temperature data in arid and semi-arid regions of Iran. Glob Planet Chang 79(1-2):1–10. https://doi.org/10.1016/j.gloplacha.2011.07.008

Verón SR, de Abelleyra D, Lobell D (2015) Impacts of precipitation and temperature on crop yields in the Pampas. Clim Chang 130:235–245. https://doi.org/10.1007/s10584-015-1350-1

Victoria RL, Martinelli LA, Moraes JM, Ballester MV, Krushche AV (1998) Surface air temperature variations in the Amazon region and its borders during this century. J Clim 11:1105–1110

Yue S, Wang C (2000) The Mann-Kendall Test modified by effective sample size to detect trend in serially correlated hydrological series. Water Resour Manag 18(3):201–218. https://doi.org/10.1023/b:warm.0000043140.61082.60

Zazulie N, and Rusticucci M (2009) Cambios en la onda anual de temperatura en el sudeste de Sudamérica In XXVIII Reunión Científica de la AAGG. La Plata. 13-17

Zhang X, Alexander LV, Hegerl GC, Klein-Tank A, Peterson TC, Trewin B, Zwiers FW (2011) Indices for monitoring changes in extremes based on daily temperature and precipitation data. Wiley Interdiscip Rev Clim Chang 2:851–870. https://doi.org/10.1002/wcc.147